arXiv:cond-mat/0207442v2 [cond-mat.supr-con] 10 Jan 2003

,

# Heavy-ion irradiation of UBe$_{13}$ superconductors

H.A. Radovan[1], E. Behne[1], R.J. Zieve[1], J.S. Kim[2], G.R. Stewart[2], W.-K. Kwok[3], and R.D. Field[4]
[1]*Physics Department, University of California at Davis*
[2]*Physics Department, University of Florida*
[3]*Argonne National Laboratory, Division of Materials Science*
[4]*Los Alamos National Laboratory,*
*Division of Materials Science and Technology*

We irradiate the heavy fermion superconductors (U,Th)Be$_{13}$ with high-energy heavy ions. Damage from the ions affects both heat capacity and magnetization measurements, although much less dramatically than in other superconductors. From these data and from direct imaging, we conclude that the irradiation does not create the amorphous columnar defects observed in high-temperature superconductors and other materials. We also find that the damage suppresses the two superconducting transitions of U$_{0.97}$Th$_{0.03}$Be$_{13}$ by comparable amounts, unlike their response to other types of defects.

PACS numbers: 74.70.Tx, 61.80.Jh

## I. INTRODUCTION

Microscopic lattice disorder can have interesting effects, particularly on unconventional superconductors. Sensitivity of the critical temperature $T_c$ to non-magnetic scatterers serves as evidence of non-$s$-wave electron-pairing. Defects can be introduced during sample fabrication, or induced afterwards by irradiation. The latter possibility encompasses both point defects created by light ions and other particles, and amorphous columns created by high-energy heavy ions. These columnar defects, which have been heavily studied in high-temperature superconductors (HTS), serve as highly efficient pinning centers for vortices and alter a sample's response to a magnetic field.

Little work has been done on another group of unconventional superconductors, the heavy fermion (HF) systems. The two orders of magnitude difference in the critical temperatures of HTS and HF superconductors changes the scale for thermal effects. Thermal fluctuations which complicate HTS behavior should be absent in HF.

The spectacular response of one heavy fermion material, UBe$_{13}$, to thorium doping makes it a good candidate for investigating other forms of lattice disorder. $T_c(x)$ is not monotonic for U$_{1-x}$Th$_x$Be$_{13}$, and a second thermodynamic phase transition appears for $0.019 < x < 0.043$ [1, 2]. No other dopant has such effects. The Be as well as the U is sensitive to substitution details. The superconducting transition is suppressed below 0.015 K for UBe$_{12.94}$Cu$_{0.06}$ [3], while the same amount of B has virtually no effect [4].

Multiple superconducting phases indicate an unconventional order parameter. A second HF material, UPt$_3$, also exhibits a double transition [5]. Furthermore, the lower phases of both UPt$_3$ and U$_{1-x}$Th$_x$Be$_{13}$ have a significantly reduced vortex relaxation rate, while in pure UBe$_{13}$ the relaxation rate is linear in temperature [6]. This may be evidence of time reversal symmetry breaking in the lower phase. If time reversal symmetry is broken, spontaneous magnetic fields can appear. Boundaries between different magnetic domains can obstruct vortex motion, leading to the observed drop in relaxation rate. Vortex motion is also reduced in U$_{1-x}$Th$_x$Be$_{13}$ for zero-field-cooling as compared to the field-cooling case [7]. Domain wall pinning may explain this effect as well, since cooling in a field should lead to larger domains and fewer domain walls. The atypical vortex behavior and the distinction between the two superconducting phases suggests that vortices may also have interesting interactions with other types of pin sites, such as columnar defects.

Here we investigate heavy-ion irradiation of (U,Th)Be$_{13}$. We show that calculations predict columnar tracks to form. However, heat capacity measurements, imaging, and magnetization measurements suggest that such tracks are not actually present. We also discuss how heavy-ion damage affects the different superconducting phases.

## II. IRRADIATION DAMAGE

The thermal spike model explains damage creation in both elements and alloys [8, 9, 10]. In this model, the heavy ion loses energy primarily to the electrons, which in turn excite phonons. The electron-phonon coupling strength $g$ determines how fast the energy is transfered to the lattice, while the thermal conductivities $\kappa_e$ and $\kappa_p$ of electrons and phonons govern how the energy spreads through the sample. The coupled differential equations

$$C_e \frac{\partial T_e}{\partial t} = \frac{\partial}{\partial r}(\kappa_e \frac{\partial T_e}{\partial r}) + \frac{\kappa_e}{r}\frac{\partial T_e}{\partial r} - g(T_e - T_p) + A(r,t)$$

$$C_p \frac{\partial T_p}{\partial t} = \frac{\partial}{\partial r}(\kappa_p \frac{\partial T_p}{\partial r}) + \frac{\kappa_p}{r}\frac{\partial T_p}{\partial r} + g(T_e - T_p)$$

describe the energy transfer. Here $\kappa_e$ and the specific heat $C_e$ of the electron system are functions of the electron temperature $T_e$, while $\kappa_p$ and the lattice specific heat $C_p$ depend on the phonon temperature $T_p$. $S_e = -\frac{dE}{dx}|_e$ is the energy loss from the heavy ion to the electrons in the target. As $S_e$ increases, a threshold value allows formation of amorphous

TABLE I: Parameters for thermal spike calculations in $\mathrm{UBe}_{13}$.

| | | |
|---|---|---|
| Debye temperature, $\Theta_D$ | 620 K | [12] |
| Melting temperature, $T_m$ | 2273 K | [13] |
| Resistivity, $\rho$ | 110 $\mu\Omega$-cm at 300 K | [14] |
| Atomic density, $n_a$ | $1 \times 10^{23}/\mathrm{cm}^3$ | [15] |
| Valence, $z$ | 2.1 | |
| $C_e$ | $4.3 \times 10^3$ erg/cm$^3$ K | |
| $C_p$ | $4.1 \times 10^3$ erg/cm$^3$ K | |
| $\kappa_e$ | $2.2 \times 10^3 T$ erg/cm K | |
| $\kappa_p$ | $9.9 \times 10^7/T$ erg/cm K | [16] |

tracks. With further increase the track radius grows. For the radial distribution of the original ion energy loss we use

$$A(r,t) \propto \frac{1}{r}\left[\frac{(1-\frac{r+\theta}{r_{max}+\theta})^{0.927}}{r+\theta}\right]$$

$$\times\left[1+\frac{K(r-L)}{M}e^{-(r-L)/M}\right]e^{-(t-t_o)^2/2t_o^2},$$

as in [11]. Here $K = 19\beta^{1/3}$, $L = 0.1$ nm, $M = (1.5+0.5\beta)$ nm, and $\beta$ is the ion velocity relative to the speed of light. The maximum range $r_{max} = 6\times10^{-6}(\frac{2mc^2\beta^2}{1-\beta^2})^{1.079}$ cm, where $m$ is the electron mass in grams and $c$ the speed of light in cm/s. The time $t_o$ is of order $10^{-15}$ s and $\theta = 9.84 \times 10^{-9}$ cm. The normalization of $A(r,t)$ is chosen so that the total energy transfer to the electrons equals $S_e$. This formula, particularly the term involving $K$, $L$, and $M$, comes from fits to observed radiation distributions in water [11]. Thermal spike calculations using these equations successfully predict the existence and even radius of columnar defects in a variety of pure metals and alloys [8].

Numerical solution of these equations requires knowledge of various parameters of the material. Table I shows the values we use. Since most of the simulation is at high temperature, we use high-temperature limits in several cases. The electronic and lattice specific heats are $C_e = 1.5k_B n_e$ and $C_p = 3k_B n_a$. The density of atoms in the lattice is $n_a$, while the electron density is $n_e = zn_a$ with $z$ the average valence of the atoms composing the material. For the electronic thermal conductivity $\kappa_e$ we use the Wiedemann-Franz law. Although in most metals the high-temperature electrical resistivity is proportional to temperature, in $\mathrm{UBe}_{13}$ the resistivity is nearly constant, so $\kappa_e$ is itself proportional to temperature [14]. For the lattice thermal conductivity $\kappa_p$ we expect a $1/T$ temperature dependence and obtain the prefactor from the 90 K value [16].

The heat of fusion of a compound equals the latent heat of its component elements, plus the difference between the liquid state mixing enthalpy and the solid enthalpy of formation. Typical values are $10^{10}$ to $10^{11}$ erg/cm$^3$. In this case the U and Be latent heats contribute $2 \times 10^{10}$ erg/cm$^3$. The heat of formation at room temperature is $-2 \times 10^{10}$ erg/cm$^3$ [13], so $4 \times 10^{10}$ erg/cm$^3$ is an upper bound on the heat of fusion. Although the mixing enthalpy is unknown, $2 \times 10^{10}$ erg/cm$^3$ is a more reasonable estimate for the heat of fusion.

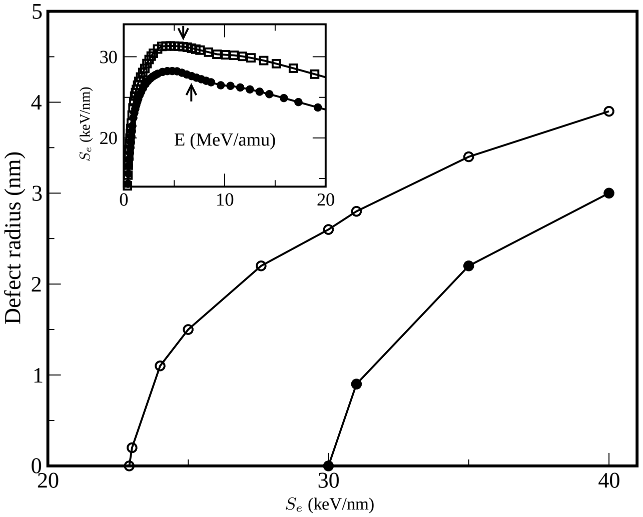

FIG. 1: Predicted defect radius in $\mathrm{UBe}_{13}$. The two curves use heat of fusion $2 \times 10^{10}$ erg/cm$^3$ (●) and $4 \times 10^{10}$ erg/cm$^3$ (○). Inset: SRIM simulation of electronic energy loss for $^{238}\mathrm{U}^{67+}$ (□) and $^{208}\mathrm{Pb}^{56+}$ (●) ions in $\mathrm{UBe}_{13}$. The arrows indicate the energy of the beams used for our irradiations.

Finally, for the electron-phonon coupling we use [8]

$$g = \frac{\pi^4 k_B^4 n_e^2 \Theta_D^2 \rho}{18L\hbar^2(6\pi^2 n_a)^{2/3}}\frac{1}{T_e}.$$

Here $L = 0.245$ erg-$\Omega$/K is the Lorentz number.

Figure 1 shows the defect radius obtained by solving the thermal spike equations numerically. The values are comparable to those of Ce and Y alloys [9], which have similar resistivity, Debye temperature, and heat of formation to $\mathrm{UBe}_{13}$. The high atomic density of $\mathrm{UBe}_{13}$ increases its sensitivity to irradiation, while the unusual temperature independence of the resistivity decreases the sensitivity.

## III. SAMPLE PREPARATION AND IMAGING

Our samples are polycrystalline $\mathrm{UBe}_{13}$ and $\mathrm{U}_{0.97}\mathrm{Th}_{0.03}\mathrm{Be}_{13}$ pieces with a grain size of about 100 $\mu$m, prepared by arc melting in an argon atmosphere and subsequent annealing at 1400° C in a beryllium atmosphere for 1000 hours [17]. Before irradiation, samples are thinned to 25 $\mu$m to prevent ion implantation, with a typical lateral dimension of 1 mm. The irradiation is performed at ATLAS, Argonne National Laboratory with 1.4 GeV $^{238}\mathrm{U}^{67+}$ and $^{208}\mathrm{Pb}^{56+}$ ions. The ion velocities are 5.9 MeV/amu and 6.7 MeV/amu, respectively. The matching fields $B_\Phi$, at which the vortex density and track density are equal, range from 0.1 T and 7 T, corresponding to typical lateral track separations from 155 to 18.5 nm. The $^{208}\mathrm{Pb}^{56+}$ ions were used for the 3 T and 7 T samples, while the $^{238}\mathrm{U}^{67+}$ were used for the

TABLE II: Effects of irradiation on transitions in (U,Th)$Be_{13}$.

| | $T_c$ (0 T) | $T_c$ (3 T) | $T_c$ (5 T) | $T_c$ (7 T) | % change at 7 T |
|---|---|---|---|---|---|
| $UBe_{13}$ | 770 | | 750 | $715^*$ | -7.1 |
| $U_{0.97}Th_{0.03}Be_{13}$ ($T_{c1}$) | 625 | $620^*$ | 613 | 530 | -15.2 |
| $U_{0.97}Th_{0.03}Be_{13}$ ($T_{c2}$) | 412 | | 400 | 345 | -16.3 |

Transition temperatures marked by (*) come from magnetization measurements, the remainder from heat capacity.

remaining samples. The irradiation takes up to two hours, depending on dosage. Because of the very small probability that two ions will reach the sample at nearly the same time and position, we assume that each ion acts independently in damaging the sample.

The inset of Figure 1 shows the electronic energy loss $S_e$ as a function of the incident beam energy, obtained from a Stopping and Range of Ions in Matter (SRIM-98 code [18]) simulation. The beam energy used for the irradiation is near the maximum and gives $S_e = 31.2$ keV/nm for uranium, $S_e = 27.6$ keV/nm for lead. The corresponding nuclear energy losses are negligible, 0.05 keV/nm and 0.04 keV/nm, respectively. The predicted stopping distances are 56 $\mu$m and 60 $\mu$m, more than twice the sample thickness. From our thermal spike calculation, the irradiation should produce defects with radius 2.8 nm (uranium) or 2.2 nm (lead).

After irradiation, both the 2.0 T $UBe_{13}$ and 7.0 T $U_{0.97}Th_{0.03}Be_{13}$ crystals were further thinned and viewed in both a Philips CM-30 transmission electron microscope (TEM) and a JEOL 3000F high resolution transmission electron microscope. The planes used for the images on the JEOL machine limited the resolution to about 0.5 nm. At $B_\Phi$ =2.0 T the defects should be about 32 nm apart. The total viewing area of about 73,000 nm$^2$ should contain about 70 defects but in fact shows no evidence of amorphous columns. For the 7.0 T sample, the imaging area of over 54,000 nm$^2$ should have nearly 200 defects. We again find no damage of radius greater than 2 nm, and only six candidates with radius from 1 nm to 2 nm. Of these, closer examination shows that three are edge dislocations. The remaining candidates could also be dislocations, viewed from angles that do not clearly show a lattice plane ending. We find no compelling reason to identify them with columnar tracks, since they do not match the expected defects either in size or in density. We conclude that columnar defects are either absent in our sample or far smaller than anticipated from our thermal spike model calculations.

We emphasize that the microscopes we used *can* detect amorphous regions of the expected size. A transmission electron microscope successfully imaged columnar defects of radius 5 nm in $UO_2$ [19]. High resolution TEM has detected columnar defects with radius down to 1 nm, for example in tin oxide [20] and $Bi_2Sr_2CaCu_2O_{8+\delta}$ [21].

## IV. HEAT CAPACITY MEASUREMENTS

We measure heat capacity on a dilution refrigerator at temperatures down to 100 mK and magnetic fields up to 8 Tesla. We use a relaxation method with a $RuO_2$ thin film thermometer, a [50:50] AuCr thin film heater, and a fine copper wire as a heat link.

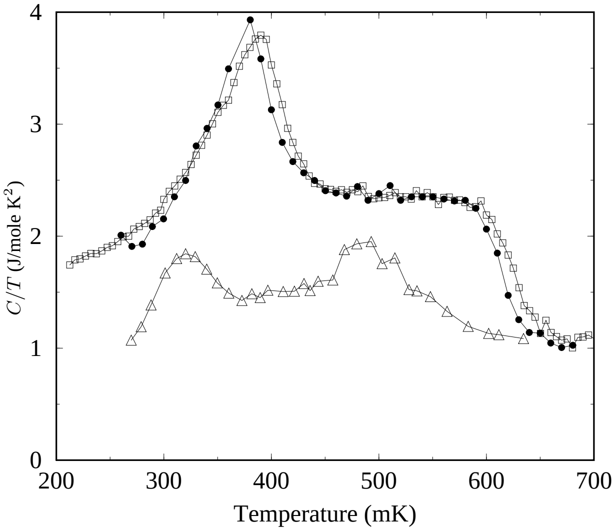

FIG. 2: Zero-field heat capacity of unirradiated (□), 5 T irradiated (●), and 7 T irradiated (△) $U_{0.97}Th_{0.03}Be_{13}$.

Figure 2 shows $C/T$ for the unirradiated, 5 T, and 7 T $U_{0.97}Th_{0.03}Be_{13}$ samples. Since we do not know the precise sample sizes, we use a multiplicative constant to set the normal state value of $C/T$ to 1.1 J/mole K$^2$ for each curve. We do not adjust the measured heat capacity for any contribution from the thermometer, heater, or mount; but comparing the curves shown to previous heat capacity measurements on bulk samples suggests that background effects are less than 30% of our signal. In any case, the background should not affect our determination of the $T_c$ suppression or transition width.

Irradiation does not measurably change $T_c$ up to $B_\Phi = 2$ T. As shown in Figure 2 for $U_{0.97}Th_{0.03}Be_{13}$, $C/T$ changes shape only slightly even at a defect density of 5 T, broadening by several mK [22]. At the higher defect density of $B_\Phi = 7$ T, the transitions do change shape. The upper transition widens by roughly a factor of two, and both decrease significantly in amplitude. Here width is defined by identifying the change in $C/T$ across the transition and using the temperature difference between the 10% and 90% values of the heat capacity. Irradiation has a similar effect on pure $UBe_{13}$, reducing $T_c$ and slightly broadening the transition, while retaining the shape of the $C/T$ curve up to 5 T. Table II summarizes the effects of irradiation on transition temperatures for both compounds. The marked transitions come from magnetization measurements rather than heat capacity, as will be discussed later.

Since the $^{208}$Pb$^{56+}$ ions used for irradiation have less energy loss than the $^{238}$U$^{67+}$ ions, they produce smaller defects in a thermal spike calculation. Depending on the value of the heat of formation, the uranium atoms might even produce defects while the lead atoms do not. We note here that the $T_c$ depression for the 3 T sample is consistent with the others. The 7 T samples have, if anything, a larger change in $T_c$ than expected from the lower irradiation dosages. Thus it appears that the $^{208}$Pb$^{56+}$ ions do as much damage as the $^{238}$U$^{67+}$ ions, despite their smaller energy loss.

It is tempting to take the nearly identical percentage suppression of the two thoriated transitions as evidence that both superconducting phases have the same pairing symmetry. However, the lower transition is between two superconducting phases, rather than between a superconducting and a normal phase. The usual arguments on how impurities affect the transition do not apply. We do note that the heavy-ion irradiation produces a different response from either non-magnetic or magnetic substitutional impurities [23]. Non-magnetic (La) impurities depress the upper transition but leave the lower transition unchanged, while magnetic (Gd) impurities suppress the lower transition more than twice as strongly as the upper one [23]. These contrasting behaviors of the two transitions for different types of defects emphasize the extreme sensitivity of the (U,Th)Be$_{13}$ system to changes in electronic structure.

The $T_c$ suppression proves that the irradiation did create some damage within the crystals. However, the small amount of suppression, like the lack of visible columns in the imaging, suggests that the damage is *not* in the form of amorphous columns. For comparison, U ions at a 2 T matching field reduce $T_c$ of YBa$_2$Cu$_3$O$_{7-x}$ by 5.3% [24], more than we find at 5 T. Although in principle our low $T_c$ reduction could occur from insensitivity to defects, rather than an absence of defects, HF superconductors are *more* sensitive than other superconductors to both neutron and light-ion irradiation [3, 25]. Even our $B_\phi = 7$ Tesla irradiation affects $T_c$ far less than the point defect work [3].

## V. MAGNETIZATION MEASUREMENTS

The motion of superconducting vortices is particularly sensitive to defects. Columnar tracks strongly pin vortices, even when the tracks are misaligned with the magnetic field by up to 40° [26]. Our imaging work could miss incomplete or misaligned columns which would be detected in a sample's magnetic behavior.

For these measurements we use bismuth Hall probes with active area $10 \times 15$ $\mu$m$^2$. We place the sample flat atop the substrate for the Hall probe. The probe measures total field at a spot near the surface of the sample, from which we extract the local magnetization of the superconductor. We typically ramp the applied magnetic field at 15 gauss per minute, and take hysteresis loops large enough to allow for full penetration. The width of the hysteresis loop, $\Delta M$, is proportional to the critical current $j_c$; and we measure both its temperature and its field dependence.

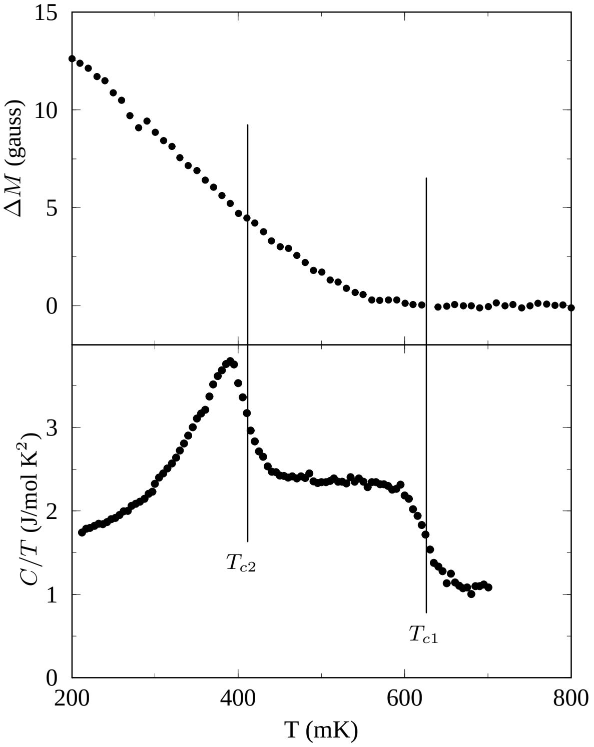

FIG. 3: Comparison of magnetization and heat capacity for unirradiated U$_{0.97}$Th$_{0.03}$Be$_{13}$. The vertical lines mark the two transitions.

Figure 3 compares hysteresis loop width and heat capacity for a sample. As $T$ increases, the hysteresis loop width decreases, closing at the same superconducting $T_c$ measured with heat capacity. For the 3 T thoriated and 7 T pure samples, the $T_c$ values in Table II are determined from magnetization rather than heat capacity data.

We note that $\Delta M(T)$ in Figure 3 shows no feature at the lower transition. By contrast, magnetic relaxation measurements show a sharp drop in the vortex creep rate at the lower transition [6]. UPt$_3$, the other HF compound with two transitions, shows the same behavior: a drop in the relaxation rate at the lower transition [6], but no feature in the magnetization itself [27]. One explanation of the difference between the two measurements is that the mechanism of vortex motion changes at the lower transition, while the pinning strength itself undergoes no sharp change. However, another possibility lies in the magnetic field history of the relaxation measurements. Vortex creep is only suppressed when the sample is exposed to a sufficiently large magnetic field, typically 1 kOe, before having the field reduced to zero for the relaxation measurements [28]. Our hysteresis loops, with maximum width of 200 Oe, may simply be in a different regime where the vortex creep shows no signature at the lower transition.

The magnetization data confirm that columnar defects are either absent or far smaller than expected. Increased pinning from the columns would appear as wider hysteresis loops, but our loop widths are comparable for unirradiated and irradiated samples. In other superconductors columnar defects produce large effects from commensurability near integral multiples of $B_\Phi$, but our hysteresis loops have no features whatsoever in $B$. One possibility is that any defects are too much smaller than 100 Å, the superconducting coherence length [14], to pin vortices.

Our magnetization measurements do show evidence of defect creation. Figure 4 shows loop width versus normalized temperature for (U,Th)Be$_{13}$ crystals of several irradiation doses, taken at zero nominal field. The width follows a power law $\Delta M(T) = \Delta M(0)(1-\frac{T}{T_c})^\alpha$ over the entire temperature range measured, approximately $0.3T_c$ to $T_c$. For the unirradiated and the 5 T samples $\alpha = 1.8$, while for the 7 T specimen $\alpha$ is reduced to 1.4. Although the magnitude agreement between the 5 T and unirradiated samples is partly coincidental, the 7 T sample has significantly the smallest $\Delta M$ observed. Both the magnitude and slope change are probably due to the damage. As with the stronger $T_c$ suppression in the 7 T sample mentioned earlier, this hints that the 5 T irradiation is a threshold for strong damage in our (U,Th)Be$_{13}$ crystals.

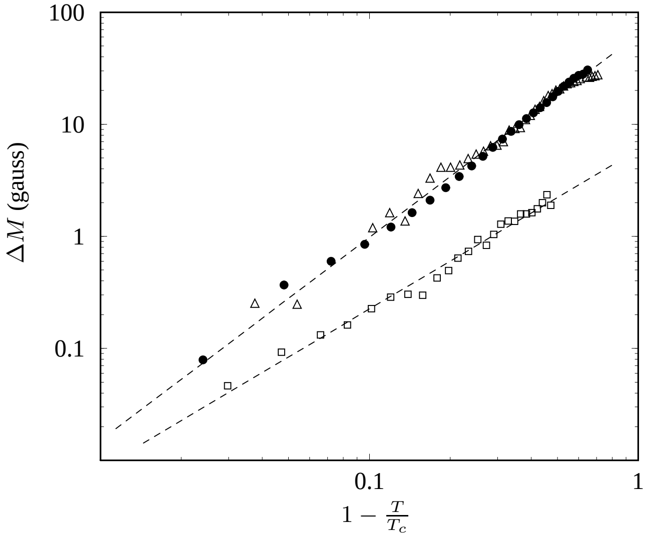

FIG. 4: Hysteresis loop width vs. reduced temperature for three thoriated samples: unirradiated (●), and irradiated with matching fields of 5 T (△) and 7 T (□).

Models for networks of superconducting grains give $\alpha = 1$ for superconductor-insulator-superconductor (SIS) tunnel junctions [29] and $\alpha = 2$ for superconductor-normal-superconductor (SNS) junctions [30]. An intermediate power law for $j_c(T)$, with $\alpha$ near 1.5, has been measured in various materials, including the HF material CeCu$_2$Si$_2$ [31]. The intermediate values may come from mixtures of SIS and SNS junctions in the samples. Similarly, the change in exponent for our 7 T sample is consistent with irradiation damage changing the characteristics of the grain network. We find the same power-law behavior in external magnetic fields up to $\mu_0 H = 2$ kG, with the exponent independent of field.

## VI. CONCLUSION

We have irradiated (U,Th)Be$_{13}$ crystals with high-energy U and Pb ions at fluences up to $B_\Phi = 7$ T. The irradiation damage reduces both superconducting transition temperatures of U$_{0.97}$Th$_{0.03}$Be$_{13}$ by over 15% for the 7 T bombardment, as well as lowering $j_c$ and reducing its temperature dependence. Unlike in previous work with substitutional impurities [23], irradiation causes a similar $T_c$ reduction for the two transitions of U$_{0.97}$Th$_{0.03}$Be$_{13}$.

Despite the measured $T_c$ reduction, transmission electron microscope and hysteresis measurements suggest that the defects are not the amorphous tracks found in HTS. Our calculations of the irradiation process predict columnar defect formation for $S_e$ down to 23 keV/nm. Our samples are irradiated above the threshold value, at $S_e \approx 30$ keV/nm. The resulting defects should have diameter 5 to 6 nm, a defect size comparable to the 10 nm superconducting coherence length. The lack of pinning by the defects and their absence from the TEM images means either that the actual radius is much smaller or that only incomplete columns or point defects form. We favor the third option. We rule out the first possibility because of the similarity between $^{208}$Pb$^{56+}$ and $^{238}$U$^{67+}$ irradiation: if the column radius were much smaller for $^{238}$U$^{67+}$ ions, then no tracks should appear at all for $^{208}$Pb$^{56+}$ ions. The lack of signal in the magnetization indicates that the sample does not have even incomplete columns, which would still pin vortices effectively. Since the reductions of $T_c$ and $j_c$ show that some damage is present, we assume we have instead created point defects.

The conditions for creation of columnar defects are important to understand, particularly as the use of such defects spreads from HTS to other materials. It is unclear whether the discrepancy between the experiment and the thermal spike calculation comes from the values chosen for the parameters or from a deeper problem with the model. The thermal spike model has successfully predicted radiation damage both in other alloys [9] and in elements, including uranium and beryllium [8]. The simplest explanation would be incorrect parameters. Although we use conservative choices, such as assuming resistivity constant rather than linear in temperature, our high-temperature extrapolations for $\rho$ or $\kappa_p$ may be incorrect. Many-electron effects produce a variety of unusual low-temperature effects in UBe$_{13}$ and other heavy fermion materials, and perhaps could influence higher-temperature behavior as well.

We also show that the lower transition of U$_{0.97}$Th$_{0.03}$Be$_{13}$ is not detectable in $j_c(T)$, despite the sharp change in magnetic relaxation rate previously observed. This may arise from differences in measurement procedure between our work and the relaxation rate studies. Another possibility is that vortices in the two superconducting phases of U$_{0.97}$Th$_{0.03}$Be$_{13}$ differ only in their behavior away from the critical current $j_c$, which magnetization measurements would not probe.

## VII. ACKNOWLEDGEMENTS

We would like to thank P.C. Canfield and J.L. Smith for fruitful discussions. This work was supported by NSF under DMR-9733898 (UCD) and by DOE under W-31-109-ENG-38 (ANL), DE-FG05-86ER45268 (Florida), and W-7405-ENG-36 (LANL).

[1] H.R. Ott, H. Rudigier, Z. Fisk, and J.L. Smith, “Phase transition in the superconducting state of $U_{1-x}Th_xBe_{13}$ ($x$ = 0-0.06),” *Phys. Rev.* **B31**, 1651 (1985).

[2] R.H. Heffner et al., “New phase diagram for (U,Th)$Be_{13}$: A muon-spin resonance and $H_{c1}$ study,” *Phys. Rev. Lett.* **65**, 2816(1990).

[3] B. Andraka et al., “Neutron irradiation of heavy-fermion superconductors,” *Phys. Rev.* **B38**, 6402 (1988).

[4] E.T. Ahrens et al., “NMR study of U(Be,B)$_{13}$ in the normal and superconducting states,” *Phys. Rev.* **B59**, 1432 (1999).

[5] R.A. Fisher et al., “Specific heat of $UPt_3$: Evidence for unconventional superconductivity,” *Phys. Rev. Lett.* **62**, 1411 (1989).

[6] A.C. Mota, E. Dumont, and J.L. Smith, “Strong vortex pinning in the low-temperature superconducting phase of ($U_{1-x}Th_x$)$Be_{13}$,” *J. Low Temp. Phys.* **117**, 1477 (1999).

[7] R.J. Zieve et al., “Anomalous flux pinning in a torus of thoriated $UBe_{13}$,” *Phys. Rev.* **B51**, 12041 (1995).

[8] Z.G. Wang, C. Dufour, E. Paumier, and M. Toulemonde, “The $S_e$ sensitivity of metals under swift-heavy-ion irradiation: A transient thermal process,” *J. Phys. Cond. Mat.* **6**, 6733 (1994).

[9] M. Ghidini et al., “Amorphization of rare earth-cobalt intermetallic alloys by swift heavy-ion irradiation,” *J. Phys. Cond. Mat.* **8**, 8191 (1996).

[10] J.P. Nozieres et al., “Swift heavy ions for magnetic nanostructures,” *Nucl. Instr. Meth.* **B146**, 250 (1998).

[11] M.P.R. Waligórski, R.N. Hamm, and R. Katz, “The radial distribution of dose around the path of a heavy ion in liquid water,” *Nucl. Tracks Radiat. Meas.* **11**, 309 (1986).

[12] G.R. Stewart, “Heavy-fermion systems,” *Rev. Mod. Phys.* **56**, 755 (1984).

[13] R. Hultgren et al., *Selected Values of the ThermodynamicProperties of Binary Alloys*, (American Society for Metals, Metals Park, OH, 1973).

[14] R.H. Heffner and M.R. Norman, “Heavy fermion superconductivity,” *Comments Cond. Mat. Phys.* **17**, 361 (1996).

[15] M.W. McElfresh et al., “Structure of the heavy-fermion superconductor $UBe_{13}$,” *Acta Cryst.* **C46**, 1579 (1990).

[16] F.G. Aliev et al., “Anisotropy of the upper critical field near $T_c$ and the properties of $URu_2Si_2$ and $UBe_{13}$ in the normal state,” *J. Low Temp. Phys.* **85**, 359 (1991).

[17] J.S. Kim, B. Andraka, and G.R. Stewart, “Investigation of the second transition in $U_{1-x}Th_xBe_{13}$,” *Phys. Rev.* **B44**, 6921 (1991).

[18] J.F. Ziegler, “The stopping and range of ions in matter (SRIM),” IBM-Research, http://www.research.ibm.com/ionbeams/.

[19] T. Wiss et al., “Radiation damage in $UO_2$ by swift heavy ions,” *Nucl. Instr. and Meth. B* **122**, 583 (1997).

[20] A. Berthelot et al., “Irradiation of a tin oxide nanometric powder with swift heavy ions,” *Nucl. Instr. and Meth. B* **166-167**, 927 (2000).

[21] N. Kuroda et al., “Effects of defect morphology on the properties of the vortex system in $Bi_2Sr_2CaCu_2O_{8+\delta}$ irradiated with heavy ions,” *Phys. Rev.* **B63**, 224502 (2001).

[22] H.A. Radovan et al., “Reduction of critical temperatures in pure and thoriated $UBe_{13}$ by columnar defects,” *Physica* **C341-348**, 1953 (2000).

[23] E.-W. Scheidt, T. Schreiner, and G.R. Stewart, “Influence of La and Gd impurities on the two phase transitions in $U_{0.97}Th_{0.03}Be_{13}$,” *J. Low Temp. Phys.* **114**, 151 (1999).

[24] L.M. Paulius et al., “Effects of 1-GeV uranium ion irradiation on vortex pinning in single crystals of the high-temperature superconductor $YBa_2Cu_3O_{7-\delta}$,” *Phys. Rev.* **B56**, 913 (1997).

[25] G. Adrian and H. Adrian, “Lattice disorder effects on superconductivity and electrical resistivity of heavy-fermion $CeCu_2Si_2$-films,” *Europhys. Lett.* **3**, 819 (1987).

[26] D.H. Kim et al., “Effect of tilted columnar defects on vortex pinning in $YBa_2Cu_3O_x$ films,” *Phys. Rev.* **B64**, 184518 (2001).

[27] E. Shung, T.F. Rosenbaum, and M. Sigrist, “Vortex pinning andstability in the low field, superconducting phases of $UPt_3$,” *Phys. Rev. Lett.* **80**, 1078 (1998).

[28] A.C. Mota, E. Dumont, J.L. Smith, and Y. Maeno, “Unconventional strong pinning in multiphase superconductors,” *Physica* **C332**, 272 (2000).

[29] V. Ambegaokar and A. Baratoff, “Tunneling between superconductors,” *Phys. Rev. Lett.* **10**, 486 (1963) and *Phys. Rev. Lett. Erratum* **11**, 104 (1963).

[30] P.G. de Gennes, “Boundary effects in superconductors,” *Rev. Mod. Phys.* **36**, 225 (1964).

[31] A. Pollini et al., “Flux dynamics and low-field magnetic properties of the heavy-fermion superconductor $CeCu_2Si_2$,” *J. Low Temp. Phys.* **90**, 15 (1993).